Theoretical investigation of pressure-induced structural transitions in americium using GGA + U and hybrid density functional theory methods

Ashok K. Verma,[1] P. Modak,[1] Surinder M. Sharma,[1] A. Svane,[2] N. E. Christensen,[2] and S. K. Sikka[3]
[1]*High Pressure and Synchrotron Radiation Physics Division, Bhabha Atomic Research Centre, Mumbai 400085, India*
[2]*Department of Physics and Astronomy, University of Aarhus, DK 8000, Aarhus C, Denmark*
[3]*Office of the Principal Scientific Adviser to Government of India, Vigyan Bhawan Annexe, Maulana Azad Road, New Delhi 110011, India*
(Received 15 May 2013; published 24 July 2013)

First-principles calculations have been performed for americium (Am) metal using the generalized gradient approximation + orbital-dependent onsite Coulomb repulsion via Hubbard interaction (GGA + U) and hybrid density functional theory (HYB-DFT) methods to investigate various ground state properties and pressure-induced structural transitions. Both methods yield equilibrium volume and bulk modulus in good agreement with the experimental results. The GGA + spin orbit coupling + U method reproduced all structural transitions under pressure correctly, but the HYB-DFT method failed to reproduce the observed Am-I to Am-II transition. Good agreement was found between calculated and experimental equations of states for all phases, but the first three phases need larger U (α) parameters (where α represents the fraction of Hartree-Fock exchange energy replacing the DFT exchange energy) than the fourth phase in order to match the experimental data. Thus, neither the GGA + U nor the HYB-DFT methods are able to describe the energetics of Am metal properly in the entire pressure range from 0 GPa to 50 GPa with a single choice of their respective U and α parameters. Low binding-energy peaks in the experimental photoemission spectrum at ambient pressure relate, for some parameter choices, well to peak positions in the calculated density of states function of Am-I.

DOI: 10.1103/PhysRevB.88.014111 PACS number(s): 71.15.Mb, 74.62.Fj, 64.70.K−

I. INTRODUCTION

Understanding the physics and chemistry of actinides at ambient and high pressures is a challenging task to both theorists and experimentalists. Experiments are problematic, mainly due to the radioactivity and toxicity of the materials. Theoretical modeling of 5f electrons, responsible for many of the properties of the actinides, is extremely difficult when they are localized.[1] Americium (Am) is the first member of the actinide series whose $5f^6$ valence electrons are localized at ambient pressure and thus do not take part in chemical bonding. But with increasing pressure, the degree of localization decreases, which results in progressive participation of these electrons in chemical bonding. This change in nature of 5f electrons has a strong influence on many physical properties, such as equation of state (EOS), phase stability, phase transitions, electrical conductivity, etc. Similar to most of the lanthanides, Am metal crystallizes in a high-symmetry, double-hexagonal, close-packed (Am-I) structure at ambient conditions. It exhibits a spectacular sequence of structural phase transitions under pressure in diamond-anvil cell experiments:[2] Under increasing pressure, Am-I transforms first to face-centered cubic (Am-II), then to the face-centered orthorhombic (Am-III) phase, and finally to the primitive orthorhombic (Am-IV). The first structural transformation is associated with a very small density change, whereas the other two phase transitions involve substantial density changes: 2% density increase during the second phase transition and 7% density increase during the third transition. The respective transition pressures are 6.1, 10.0, and 16.1 GPa (Ref. 2). The Am-III crystal structure is the same as the gamma phase of plutonium.[2] The Am-IV phase was also proposed in plutonium at pressures higher than 37 GPa (Ref. 3). The ambient electrical resistivity (68 $\mu\Omega$ cm) of Am is similar to values found for ordinary metals, but under pressure, the resistivity of Am increases very much, reaching a value of 500 $\mu\Omega$ cm in its fourth phase.[4]

Since strong correlations related to 5f electron localization are not accurately described by the local density approximation (LDA) and the generalized gradient approximation (GGA) of the standard density functional theory (DFT) that are based on the homogeneous electron gas, various strategies have been adopted to include such effects in the calculations.[5–10] In the simplest approach, the effects of strong correlations were simulated through exchange interaction by inclusion of magnetic order in the standard DFT calculations.[5–7] This approach was very successful in reproducing the ground state volume, bulk modulus, and phase transition sequence under pressure in Am. However this simple approach did not reproduce many other important properties, including photoemission data, phase transition pressures, and associated volume collapse on the phase transitions.[5–7] Further, this approach incorrectly predicts a magnetic ground state for the nonmagnetic Am (Refs. 5–7). The inclusion of self-interaction corrections in LDA also describes the 5f localization transition in the actinide metals series.[10]

Some of the most popular methods used for strongly correlated systems are DFT + U and dynamical mean-field theory (DMFT). Basically, in these methods the electron localization is realized by applying orbital-dependent onsite Coulomb repulsion via Hubbard interaction (U) between the chosen electrons.[8,9] DFT + U treats this added term in the mean field limit, while DMFT allows a more advanced treatment of the Hubbard term depending on the impurity solver involved.[9,11] These methods were successfully applied in calculating the ground state volume, bulk modulus, and electronic properties of Am (Refs. 12–15). Although the DMFT (or DFT + DMFT as in Ref. 12) method was able to reproduce the pressure-driven structural transition sequence correctly, the calculated EOS,

specifically for the Am-III phase, did not show a good match to experimental data.[12] This work did not list the values of transition pressures and associated volume collapses. So far, pressure-driven phase transitions in Am have not been investigated using the DFT + U method.

It is important to mention that DFT + U and DMFT are not truly first-principles methods since one has to either fine-tune the Hubbard parameter U for a given phase with some known property or one has to evaluate it by means of constrained DFT calculations[16–18] or by a self-consistent linear response method.[19] Also, it is not meaningful to compare total energies of different structures if they have different U values. So, to study the structural phase transitions, one has to assume that the U parameter remains unchanged not only in different structures, but also when the pressure is varied. This strategy is applied in this work.

Hybrid density functional theory (HYB-DFT) is another approach that was recently developed to treat the localized electrons. In this approach an approximate DFT exchange energy functional is mixed with the exact Hartree-Fock (HF) exchange energy [i.e., $E_{XC}^{\mathrm{HYB}} = E_{XC}^{\mathrm{DFT}} + \alpha(E_X^{\mathrm{HF}} - E_X^{\mathrm{DFT}})$], where α represents the fraction of HF exchange energy replacing the DFT exchange energy.[20] In this method, different α parameters represent different exchange-correlation functionals. This method was successfully applied in calculating the ground state properties of many strongly correlated systems, such as UO_2, δ-Pu, and Am-I (Refs. 21–24), but so far it has not been applied to prediction of structural phase transitions of any system which requires very accurate relative energies.

A separate approach to describe the electronic structure of actinide systems is provided by the GW approach,[25] where G refers to the solid Green's function and W denotes the dynamically screened electron-electron interaction. Applications to actinides revealed a significant narrowing and renormalization of 5f electrons.[26–28]

This paper reports results of calculations of ground state properties, pressure-driven structural transformation, and EOS of Am metal using GGA + SO + U (SO, spin-orbit coupling) and HYB-DFT methods. In the GGA + SO + U calculations the U parameter was varied from 3.0 eV to 5.5 eV, whereas in HYB-DFT calculations the α parameter was varied from 0.15 to 0.50. Both of these methods reproduced the experimental ground state volume and bulk modulus well. The GGA + SO + U method reproduces all pressure-induced structural transition correctly, whereas the HYB-DFT method fails to produce the Am-I to Am-II transition. The first three phases need larger U (α) parameters than the last phase to match experimental pressure-volume data, indicating the partial delocalization of the 5f states in the fourth phase.

The methods used in this work are described in Sec. II, whereas details of the results summarized above are given in Sec. III, which also briefly discusses possible relations between the calculated band structures and photoemission spectra.

TABLE I. Ground state atomic volume and bulk modulus of double-hexagonal close-packed Am. Data in parentheses is from Refs. 13 and 23, and data shown with an asterisk (*) is from Ref. 5. Here, NM and AFM refer to nonmagnetic and antiferromagnetic calculations, respectively.

	V_0 (Å^3)	B_0 (GPa)	B_0'
NM GGA	17.3	155.3	5.6
NM GGA + SO	19.6	68.9	7.1
	(20.4)	(66.6)	
	28.8	30.5	2.8
AFM GGA + SO	29.7*	25.6*	
	(29.3)	(28.2)	
NM GGA + SO + U (=3.0 eV)	26.4	31.9	4.5
NM GGA + SO + U (=3.5 eV)	27.7	31.7	3.5
	(29.3)	(35.1)	
NM GGA + SO + U (=4.0 eV)	28.7	34.9	2.9
	(29.9)	(42.5)	
NM GGA + SO + U (=4.5 eV)	29.4	37.0	2.9
	(30.8)	(49.1)	
NM HYB-DFT ($\alpha = 0.15$)	25.6	40.7	4.0
	(27.3)	(40.0)	
NM HYB-DFT ($\alpha = 0.19$)	27.1	38.1	4.3
NM HYB-DFT ($\alpha = 0.25$)	28.7	43.3	3.8
	(30.0)	(42.0)	
NM HYB-DFT ($\alpha = 0.50$)	31.1	43.3	2.4
LDA + DMFT ($U = 4.5$ eV)[12]	27.4	45.0	
Expt.[2]	29.3	29.7 ± 1.5	3.7 ± 0.2

II. METHODOLOGY

All calculations were done using the DFT-based full-potential linear-augmented plane wave (FP-LAPW) method as implemented in the WIEN2k computer program.[29] In the FP-LAPW method, the charge density and the crystal potential can have arbitrary shape, and the wavefunctions are variationally approximated to the true wavefunctions in the region of fixed energies E_v. Core electrons are treated relativistically by solving the Dirac equation, and valence electrons are treated semirelativistically by including SO interactions in the second-variational approach. Most of the calculations were done with a nonmagnetic state as, experimentally, Am is known to be a nonmagnetic metal; also, a good match of theoretical and experimental photoemission data was found only for this state.[13,14]

An augmented plane wave (APW) + lo basis was used to describe 6d and 5f states, and a LAPW basis was used to describe 6s, 6p, and all higher angular momentum states up to $l_{\max} = 10$ in the expansion of the electronic wave functions. Additional local orbitals were added to the 6s and 6p semicore states. The basis set was further extended by including the $p_{1/2}$ relativistic local orbitals for a better description of the 6p state.[30] The muffin-tin radius was taken equal to 2.25 Bohr (1 Bohr = 0.529 177 Å), and $R_{\mathrm{MT}} * K_{\mathrm{MAX}}$ was set equal to 11. Full Brillouin zones were sampled by 2500 (for Am-I, Am-III, and Am-IV) and 5000 (for Am-II) points. An 8-Ry energy cutoff was used for the second-variational approach of SO interactions. Exchange correlation was treated within the generalized gradient approximation (GGA; Ref. 31). Onsite Hubbard interaction between the 5f electrons was treated within the fully rotationally invariant version.[8] Here, U (equal to what is often called $U_{\mathrm{eff}} = U - J$) is taken as the on-site interaction term as suggested in Ref. 24.

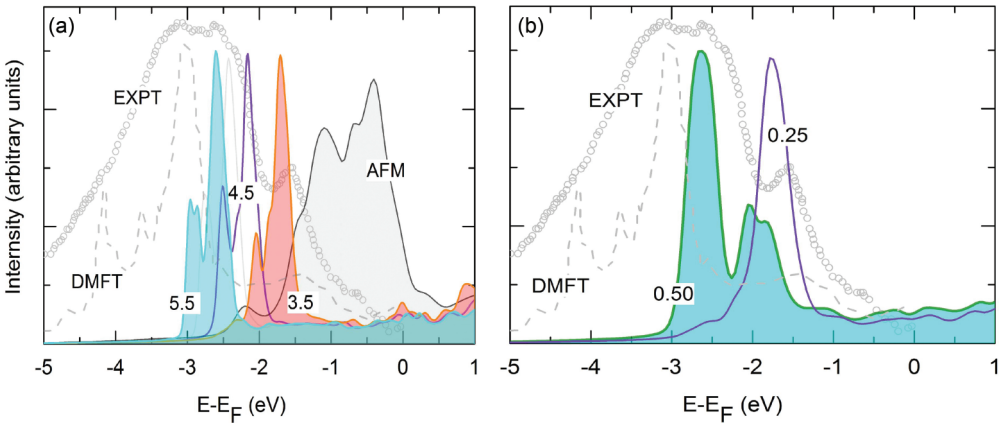

FIG. 1. (Color online) (a) The GGA + SO + U and (b) HYB-DFT density of state (DOS) functions of double-hexagonal close-packed Am at the experimental equilibrium volume (Ref. 2). Corresponding U values (eV) and α parameters are given on the curves. The light gray curve shows the DOS function for $U = 4.5$ eV with $R_{MT} = 2.6$ Bohr, same as in Ref. 13. The experimental photoemission spectrum was traced from Ref. 33, and the LDA + DMFT DOS data (for the face-centered cubic structure) was traced from Ref. 12.

III. RESULTS AND DISCUSSION

A. Ground state properties

Table I presents the calculated ground state quantities together with previous theoretical and experimental data. The nonmagnetic GGA is unable to yield the ground state volume and bulk modulus accurately. Although the volume and bulk modulus data improve with inclusion of SO, the data mismatch is still unacceptable: Volume and bulk modulus differ from experiments[2] by -31% and 132%, as also found in previous studies.[5,6] In fact, this mismatch was expected since standard DFT with GGA treats the $5f$ electrons as itinerant (i.e., they take part in the chemical binding). For example, the GGA provided a good description of various properties of ThN and UN in which $5f$ electrons are itinerant.[32] Similar to the previous work,[5,6] the GGA + SO calculations with antiferromagnetic (AFM) order reproduce the ground state volume and bulk modulus data extremely well but fail to reproduce the photoemission spectrum[33] [see Fig. 1(a)].

As expected, incorporation of onsite Coulomb repulsion via Hubbard interaction between the $5f$ electrons in the calculations resulted in great improvement in the ground state

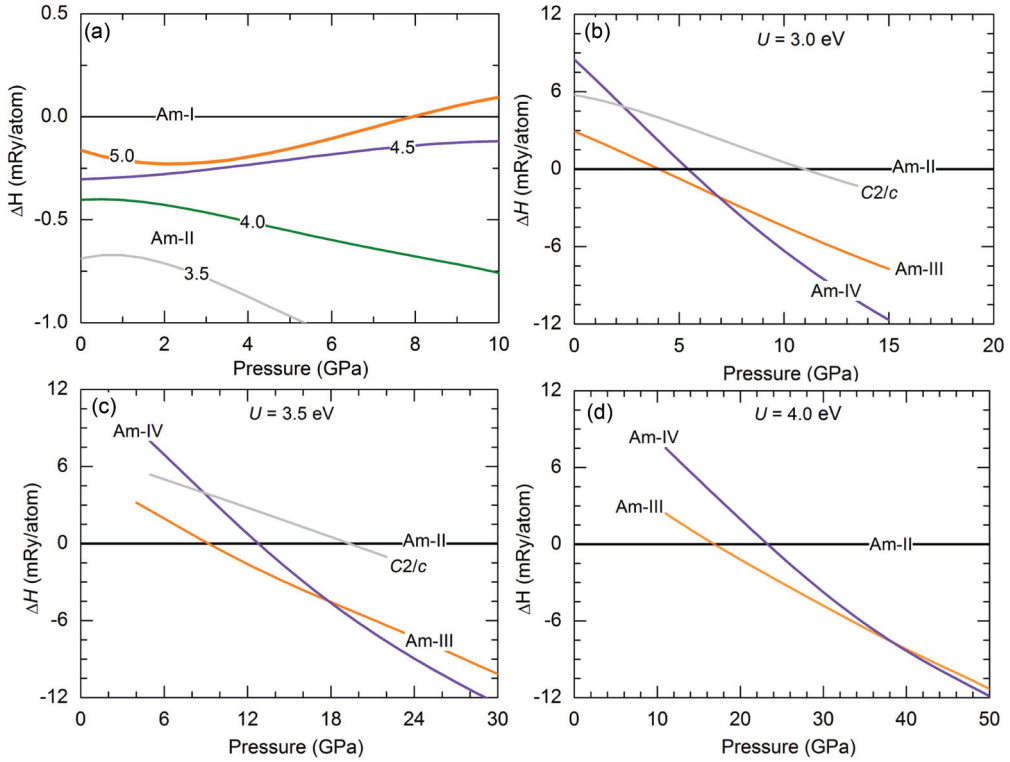

FIG. 2. (Color online) Variation of relative enthalpies of different phases of Am with pressure in the GGA + SO + U. (a) The enthalpy of Am-II relative to Am-I is shown for several values of U (eV). (b)–(d) The enthalpies of the Am-III, Am-IV, and $C2/c$ phases are shown relative to the Am-II phase for $U = 3.0$, 3.5, and 4.0 eV.

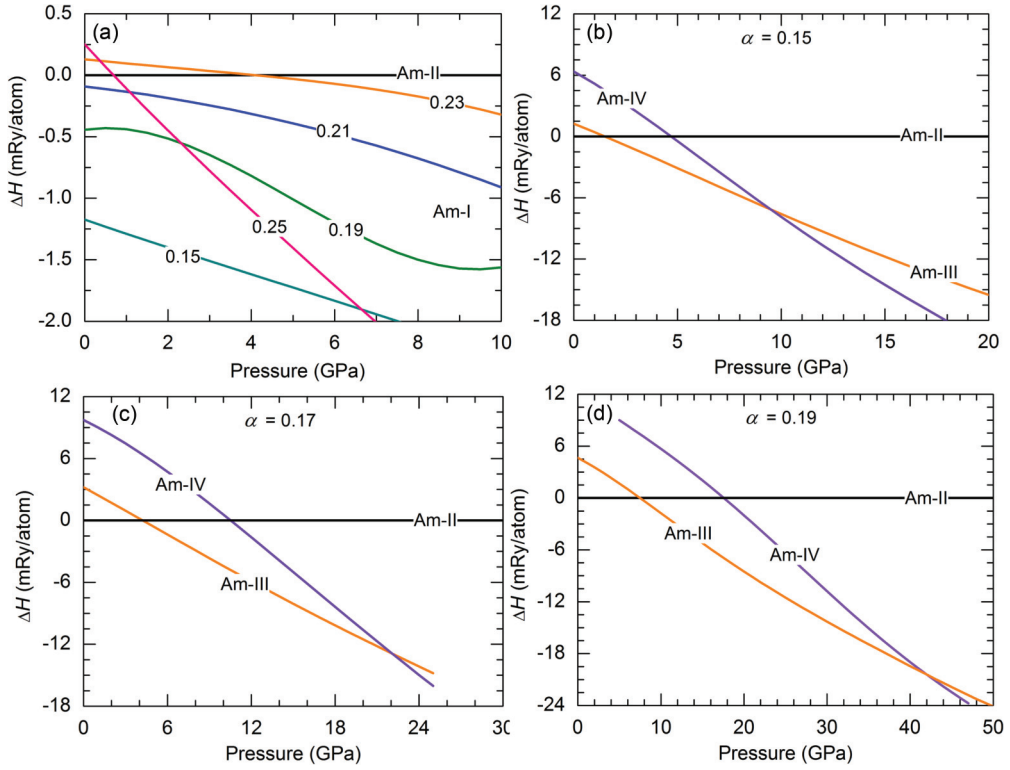

FIG. 3. (Color online) Variation of relative enthalpies of different phases of Am with pressure in the HYB-DFT method. (a) The enthalpy of Am-II relative to Am-I is shown for several values of the α parameter. (b)–(d) The enthalpies of the Am-III and Am-IV phases are shown relative to the Am-II phase for $\alpha = 0.15$, 0.17, and 0.19.

properties; for example, the difference between calculated and experimental volumes reduces to less than 10% for $U = 3.0$ eV, and this difference further reduces as U increases (see Table I). The calculated volume and bulk modulus are in good agreement with the experimental results for all three U (=3.5, 4.0, and 4.5 eV) values. The volume increases and the bulk modulus decreases relative to nonmagnetic GGA values. This is a direct consequence of the $5f$ electron localization, which increases with increasing U. Figure 1(a) shows the total density of state (DOS) functions for $U = 3.5$, 4.5, and 5.5 eV together with an experimental photoemission spectrum. Unlike volume and bulk modulus data, the DOS functions agree with experimental photoemission spectra[33] reasonably well only when U is taken to be 5.5 eV, and then only when the spectral positions of peaks at low binding energies are compared with peaks in the DOS. A similar trend was also noticed in earlier work.[13] A much better relation was found between the photoemission spectrum and the spectral function from the DMFT calculation.[12] The usual band structure picture breaks down in the DMFT, which produces a spectral function containing incoherent features, minor multiplet transitions,[9,12,15] not directly related to bands.

TABLE II. Calculated phase transition pressures and percent volume collapse ($\Delta V/V$) on phase transitions. Here, NM and AFM refer to nonmagnetic and antiferromagnetic calculations, respectively.

	Am-II → Am-III		Am-III → Am-IV	
	P (GPa)	$\Delta V/V$(%)	P (GPa)	$\Delta V/V$(%)
NM GGA + SO + U (=3.0 eV)	4.0	6.8	6.9	6.8
NM GGA + SO + U (=3.5 eV)	9.3	5.7	17.6	3.8
NM GGA + SO + U (=4.0 eV)	16.8	4.6	38.6	1.1
NM HYB-DFT ($\alpha = 0.15$)	1.5	7.8	9.53	6.3
NM HYB-DFT ($\alpha = 0.17$)	4.3	7.0	22.1	4.7
NM HYB-DFT ($\alpha = 0.19$)	7.4	6.4	42.2	3.0
Previous AFM				
GGA + SO[5]	18.6	10.0	19.8	10.0
GGA + SO + OP[6,a]	10.7		15.8	
Expt.[2]	10.1	2.0	16.0	7.0

[a]OP: orbital polarization.

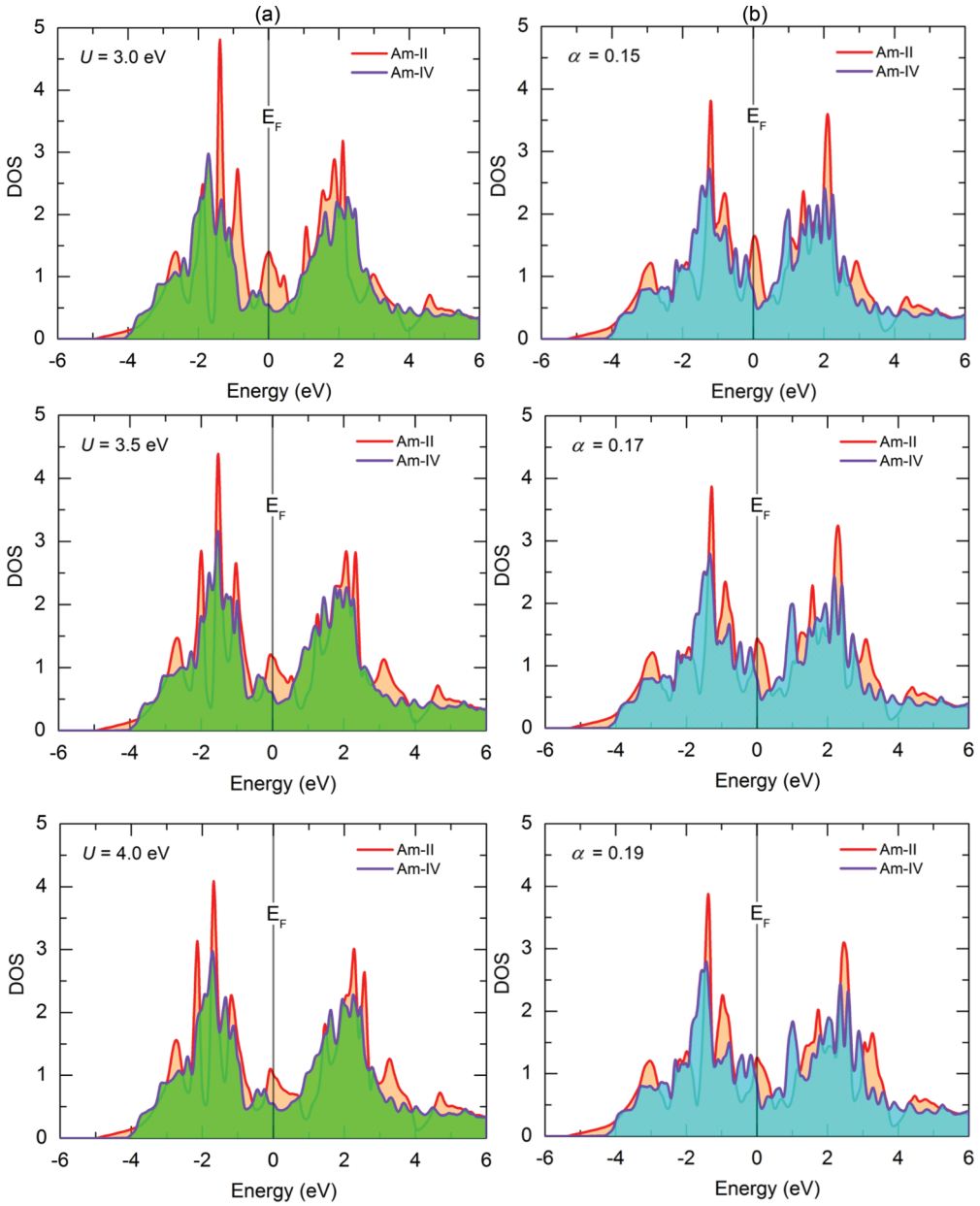

FIG. 4. (Color online) DOS ($eV^{-1}\cdot spin^{-1}$) functions calculated with (a) GGA + SO + U and (b) HYB-DFT methods in the Am-IV stability region (atomic volume = 16.70 Å^3). In all cases the high peak at E_F seen in the Am-II phase is split in the transformation to Am-IV.

Similar to the GGA + SO + U method, the HYB-DFT method also improves the description of ground state properties with an increasing α parameter. Here a set of α values were tried from 0.15 to 0.50, and the results of a few selected cases are presented in Table I. The volume and bulk modulus values match reasonably well with experimental results for all α values except $\alpha = 0.15$, for which volume differs by -12%. Figure 1(b) depicts the calculated DOS functions together with an experimental photoemission spectrum. Also here it is seen that the band-structure calculations cannot be applied to predict even roughly the peak positions in photoemission spectra.

B. Structural stability under pressure

Figures 2 and 3 show the calculated phase diagram under pressure for Am at 0 K. Both methods correctly reproduce the experimental structural phase transition sequence: face-centered cubic (Am-II) to face-centered orthorhombic (Am-III) to primitive orthorhombic (Am-IV). However, as the Hubbard parameter (U) increases from 3 eV to 4 eV, the phase transition pressures shift toward higher pressure values. Table II lists estimated transition pressure along with associated volume change for different U values. All U parameters are able to reproduce the phase transition sequence correctly, but the transition pressures and total volume collapse (Am-II to Am-IV transition) matches well with experimental results for $U = 3.5$ eV. A much larger total volume collapse was predicted in previous calculations.[5] The stability of the monoclinic structure, which was observed in Cm between the face-centered cubic and the face-centered orthorhombic structures,[34] was also studied, but it was not found stable. Similar structural trends were also found with HYB-DFT

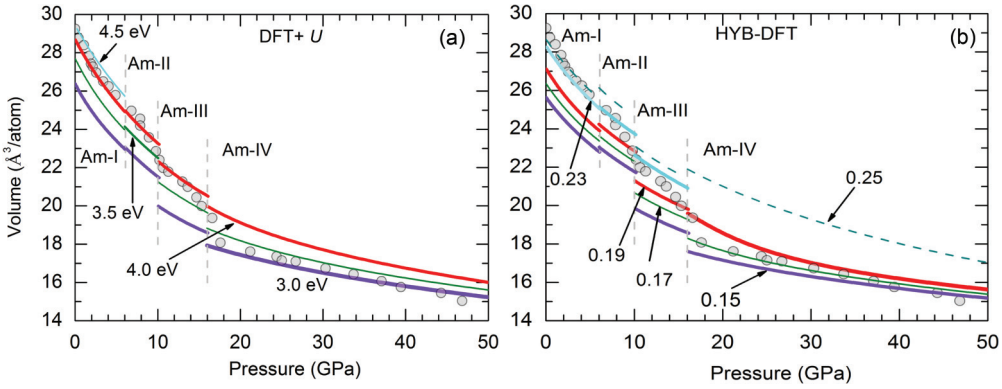

FIG. 5. (Color online) Calculated EOS of Am metal in different phases. Filled circles represent the experimental data (Ref. 2). Vertical dashed lines represent the experimental phase boundaries. (a) Results for four different values. (b) The α parameter is varied between 0.15 and 0.25.

calculations, and the corresponding phase transition pressures and volume collapses are given in Table II.

The phase stability relation of Am-I and Am-II structures show interesting behavior under pressure in both methods. Although the GGA + SO + U approximation predicts Am-I structure as the ground state phase for all U values [see Fig. 2(a)], the transition to Am-II was found only for U = 5.0 eV with a reasonable transition pressure (~7.9 GPa). For U = 3.5 eV and 4.0 eV, the Am-I structure becomes progressively more stable with pressure. The HYB-DFT method predicts Am-I as the ground state phase for all α values below 0.21 [see Fig. 3(a)]. For α values larger than 0.21 the calculations incorrectly predict Am-II as the ground state, but the Am-I structure becomes stable at higher pressures. It must be noted that in an ideal setting, the double-hexagonal close-packed structure differs from the face-centered cubic structure only in the stacking sequence of the atomic planes. This may be one of the reasons for the small enthalpy differences seen here between these two structures.

Söderlind *et al.*[35] have shown that low-symmetry structures such as tetragonal, orthorhombic, monoclinic, etc. in the light actinides are stabilized by Peierls-type symmetry lowering distortions of the high-symmetry structures. These distortions remove the degeneracy of the narrow 5f bands positioned at the Fermi level, leading to reduced DOS at the Fermi level, which in turn lowers the band structure contribution to the total energy. This mechanism is found to work in stabilization of the lower symmetry Am-IV phase over the higher symmetry Am-II phase, as illustrated in Fig. 4. Here, a substantial reduction in DOS at the Fermi level is seen in the Am-IV phase relative to the Am-II phase for all chosen U and α parameters.

Figure 5 shows calculated pressure-volume relations up to 50 GPa for various U and α parameters. Both methods are able to reproduce the experimental data extremely well. The first three phases need larger U and α parameters than the last phase to match the experimental EOS. Clearly, the 5f electrons are least correlated in the fourth phase.

IV. CONCLUSIONS

In summary, we have studied Am metal at ambient and high pressures using GGA + SO + U and HYB-DFT methods. The calculated ground state properties show fairly good agreement with the experimental data. The GGA + SO + U method predicts all structural transitions correctly, but the HYB-DFT method fails to predict the Am-I to Am-II transition. The transition from Am-I to Am-II needs a larger U parameter than the other transformations. Extremely good matches between theoretical and experimental EOS data are found for all phases, but in some cases different phases need different U (α) parameters. The first three phases need larger U (α) parameters than the fourth phase in order to match the experimental EOS data. We would like to emphasize that neither the GGA + U nor the HYB-DFT methods are able to treat Am metal properly with a single choice of parameters in the entire pressure range from 0 GPa to 50 GPa. Thus, further methodology development is needed to describe Am metal properly under high pressure.

[1] K. T. Moore and G. van der Laan, Rev. Mod. Phys. **81**, 235 (2009).
[2] S. Heathman, R. G. Haire, T. Le Bihan, A. Lindbaum, K. Litfin, Y. Méresse, and H. Libotte, Phys. Rev. Lett. **85**, 2961 (2000).
[3] S. K. Sikka, Solid State Commun. **133**, 169 (2005).
[4] J.-C. Griveau, J. Rebizant, G. H. Lander, and G. Kotliar, Phys. Rev. Lett. **94**, 097002 (2005).
[5] M. Pénicaud, J. Phys.: Condens. Matter **17**, 257 (2005).
[6] P. Söderlind and A. Landa, Phys. Rev. B **72**, 024109 (2005).
[7] P. Söderlind, K. T. Moore, A. Landa, B. Sadigh, and J. A. Bradley, Phys. Rev. B **84**, 075138 (2011).
[8] V. I. Anisimov, I. V. Solovyev, M. A. Korotin, M. T. Czyzyk, and G. A. Sawatzky, Phys. Rev. B **48**, 16929 (1993).
[9] A. Georges, G. Kotliar, W. Krauth, and M. J. Rozenberg, Rev. Mod. Phys. **68**, 13 (1996).
[10] A. Svane, L. Petit, Z. Szotek, and W. M. Temmerman, Phys. Rev. B **76**, 115116 (2007).
[11] G. Kotliar, S. Y. Savrasov, K. Haule, V. S. Oudovenko, O. Parcollet, and C. A. Marianetti, Rev. Mod. Phys. **78**, 865 (2006).
[12] S. Y. Savrasov, K. Haule, and G. Kotliar, Phys. Rev. Lett. **96**, 036404 (2006).

[13]M. F. Islam and A. K. Ray, Solid State Commun. **150**, 938 (2010).
[14]A. K. Verma, P. Modak, S. M. Sharma, and S. K. Sikka, Solid State Commun. **164**, 22 (2013).
[15]A. Svane, Solid State Commun. **140**, 364 (2006).
[16]V. I. Anisimov and O. Gunnarsson, Phys. Rev. B **43**, 7570 (1991).
[17]J. Zaanen, O. Jepsen, O. Gunnarsson, A. T. Paxton, and A. Svane, Physica C **153–155**, 1636 (1988).
[18]M. S. Hybertsen, M. Schlüter, and N. E. Christensen, Phys. Rev. B **39**, 9028 (1989).
[19]M. Cococcioni and S. de Gironcoli, Phys. Rev. B **71**, 035105 (2005).
[20]A. D. Becke, J. Chem. Phys. **98**, 1372 (1993).
[21]K. N. Kudin, G. E. Scuseria, and R. L. Martin, Phys. Rev. Lett. **89**, 266402 (2002).
[22]R. Atta-Fyn and A. K. Ray, Europhys. Lett. **85**, 27008 (2009).
[23]R. Atta-Fyn and A. K. Ray, Chem. Phys. Lett. **482**, 223 (2009).
[24]I. D. Prodan, G. E. Scuseria, and R. L. Martin, Phys. Rev. B **76**, 033101 (2007).
[25]L. Hedin, Phys. Rev. **139**, A796 (1965).
[26]A. N. Chantis, R. C. Albers, A. Svane, and N. E. Christensen, Philos. Mag. **89**, 1801 (2009).
[27]A. Kutepov, K. Haule, S. Y. Savrasov, and G. Kotliar, Phys. Rev. B **85**, 155129 (2012).
[28]A. Svane, R. C. Albers, N. E. Christensen, M. van Schilfgaarde, A. N. Chantis, and Jian-Xin Zhu, Phys. Rev. B **87**, 045109 (2013).
[29]P. Blaha, K. Schwarz, G. K. H. Madsen, D. Kvasnicka, and J. Luitz, *WIEN2k, an Augmented Plane Wave + Local Orbitals Program for Calculating Crystal Properties* (Karlheinz Schwarz, Techn. Universität Wien, Austria, 2001).
[30]J. Kunes, P. Novak, R. Schmid, P. Blaha, and K. Schwarz, Phys. Rev. B **64**, 153102 (2001).
[31]J. P. Perdew, K. Burke, and M. Ernzerhof, Phys. Rev. Lett. **77**, 3865 (1996).
[32]P. Modak and A. K. Verma, Phys. Rev. B **84**, 024108 (2011).
[33]T. Gouder, P. M. Oppeneer, F. Huber, F. Wastin, and J. Rebizant, Phys. Rev. B **72**, 115122 (2005).
[34]S. Heathman, R. G. Haire, T. Le Bihan, A. Lindbaum, M. Idiri, P. Normile, S. Li, R. Ahuja, B. Johansson, and G. H. Lander, Science **309**, 110 (2005).
[35]P. Söderlind, O. Eriksson, B. Johansson, J. M. Wills, and A. M. Boring, Nature (London) **374**, 524 (1995).